Processing and Application of Ceramics 13 [3] (2019) 281–286
https://doi.org/10.2298/PAC1903281A



# Structure and electrical properties of Eu-doped $SrBi_2Nb_2O_9$ ceramics

Mohamed Afqir[1,2,*], Amina Tachafine[2], Didier Fasquelle[2], Mohamed Elaatmani[1], Jean-Claude Carru[2], Abdelouahad Zegzouti[1], Mohamed Daoud[1], Abdelhamid Oufakir[1]

[1]*Laboratoire des Sciences des Matériaux Inorganiques et leurs Applications, Faculté des Sciences Semlalia, Université Cadi Ayyad, Marrakech, Morocco*

[2]*Unité de Dynamique et Structure des Matériaux Moléculaires, Université du Littoral- Côte d'Opale, Calais, France*

Received 25 February 2019; Received in revised form 15 May 2019; Accepted 7 August 2019

## Abstract

*Structure and dielectric properties of Eu-doped $SrBi_2Nb_2O_9$ ceramics (with 0, 20 and 35 at.% of Eu), prepared by the solid-state method and sintering, were investigated. XRD, FTIR and SEM measurements were provided to validate the characteristic structural features of the obtained ceramics. For all samples, the orthorhombic structure was identified through XRD analysis. SEM results confirmed that the fabricated samples have relatively dense structure with rod- and plate-like grains typical for Aurivillius layered structures. Dielectric results showed that the doping with Eu decreases dielectric constant and reduces dielectric loss. Movement of the dielectric peak towards higher temperatures appearing at about 400 °C with increase of frequency indicates on relaxor behaviour of the sample with 35 at.% of Eu.*

***Keywords:*** *$SrBi_2Nb_2O_9$, ceramics, microstructure, dielectric*

## I. Introduction

$SrBi_2Nb_2O_9$ is a member of Aurivillius family and have a generic formula of $(Bi_2O_2)^{2+}(A_{n-1}B_nO_{3n+1})^{2-}$, where A represents mono-, di- or trivalent ions, B represents for tri-, tetra-, penta- or hexavalent ions and $n$ describes a number of pseudo-perovskite ($A_{n-1}B_nO_{3n+1}$) interleaved between two ($Bi_2O_2$) layers [1]. Because of their low remnant polarization, high leakage and polarization fatigue, $SrBi_2Nb_2O_9$ (same as $SrBi_2Ta_2O_9$) is now favourite candidate for FeRAM technologies [2,3]. However, these materials suffer from bismuth vacancies accompanied with oxygen vacancies. Rare earth cations isovalent substitution for $Bi^{3+}$ has been found to be able to suppress oxygen vacancies [4]. Recently, we had demonstrated that the partial substitution of bismuth by samarium, cerium and holmium leads to a significant decrease in dielectric loss [5–7]. Moreover, by reaching up to 40 and 50 mol% of samarium, relaxor behaviour took place. Studies on Eu-doped $SrBi_2Nb_2O_9$ have been prioritized mainly for optical properties and restricting dielectrics were not a key focus. Thus, $Eu^{3+}$ presents some characteristic properties enabling it to be frequently used as a probe [8,9]. To our knowledge, electrical and dielectric properties of Eu-doped $SrBi_2Nb_2O_9$ ceramics have not been discerned. In this regard, we study here $SrBi_{2-x}Eu_xNb_2O_9$ ($0 \le x \le 0.35$) ceramics by using XRD, FTIR, SEM characterization and dielectric measurements.

## II. Experimental

$SrBi_{2-x}Eu_xNb_2O_9$ ceramic powders (where $x$ = 0, 20 and 35 at.%) were synthesized by mixing stoichiometric amounts of $Bi_2O_3$, $SrCO_3$, $Nb_2O_5$ and $Eu_2O_3$ (99% Rectapur™), $SrCO_3$ (98% Aldrich), $Nb_2O_5$ (99.5% Acros Organics) and $Eu_2O_3$ (99.9% Rectapur®) in ethanol for one hour using an agate mortar. The mixtures were calcined at 1100 and 1200 °C for 12 h for the undoped and doped samples, respectively. The calcined powders were again ground with additional 5 mol% of $Bi_2O_3$ and then uniaxially pelleted at 1 MPa. The pressed pellets were sintered at 1130 and 1230 °C for 12 h for the undoped and doped samples, respectively. Two sintering temperatures were used to provide diffusion-bonding, which after cooling generates a desired structure.

* Corresponding author: tel: +212642379483,
e-mail: *mohamed.afqir@yahoo.fr*

Powder X-ray diffraction (XRD) patterns were collected by a diffractometer of the (Philips Company with X'Pert Pro) using monochromatized $CuK_\alpha$ radiation ($\lambda$ = 1.54 Å). FTIR spectra were recorded on KBr pellets using a Bruker Vertex 70 DTGS Fourier transform infrared spectrometer with a resolution of 4 $cm^{-1}$ in the range of 400 to 4000 $cm^{-1}$. Structure and morphology of the products were studied using SEM (EDAX AMETEK) with secondary electron detector and high voltage of 20 kV. The dielectric properties were investigated in temperature range from 20–500 °C using LCR meter HP 4284A.

## III. Results and discussion

### 3.1. Structural characterization

XRD patterns of the calcined $SrBi_{2-x}Eu_xNb_2O_9$ ($x$ = 0, 0.2, 0.35) ceramic powders are shown in Fig. 1. All samples were compatible with the diffractogram of $SBi_2Nb_2O_9$ with orthorhombic structure (01-086-1190). The peak at 29.1° was assigned to the diffraction plane (115). For this peak, the crystallite sizes estimated by the Debye-Scherrer's formula [10] are 48, 29 and 25 nm for $x$ = 0, 0.2 and 0.35, respectively. From Fig. 2, it can be observed that there is a slight shift of XRD 115 peak towards higher $2\theta$ values with the increase of Eu-content. This may be due to the compression in crystal structure and decrease of the unit cell volume with increasing the value of $x$, since europium ion (0.95 Å) is smaller than bismuth ion (1.02 Å) [11]. The present results confirm that $Eu^{3+}$ ions diffused into the crystal lattice of $SrBi_2Nb_2O_9$ and formed a stable solid solution with $SrBi_2Nb_2O_9$. Theoretical density of the samples can be determined from XRD data using:

$$d = \frac{n \cdot M}{N \cdot V} \tag{1}$$

where $M$ is the molecular weight, $n$ is the number of molecules per unit cell, $V$ is the volume of unit cell and $N$ is Avogadro's number. Calculated density was found

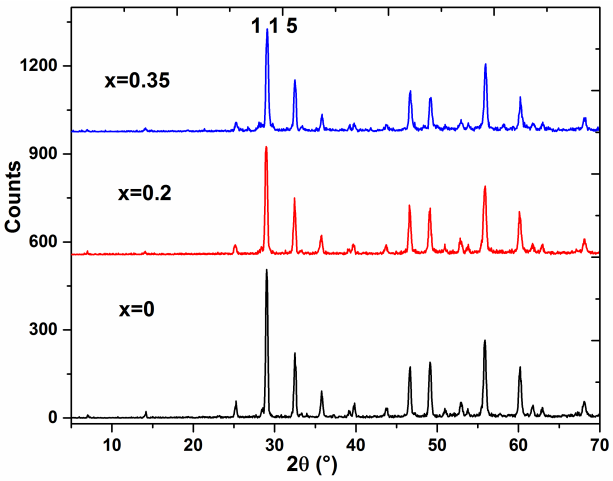


**Figure 1. XRD patterns of $SrBi_{2-x}Eu_xNb_2O_9$ ceramic**

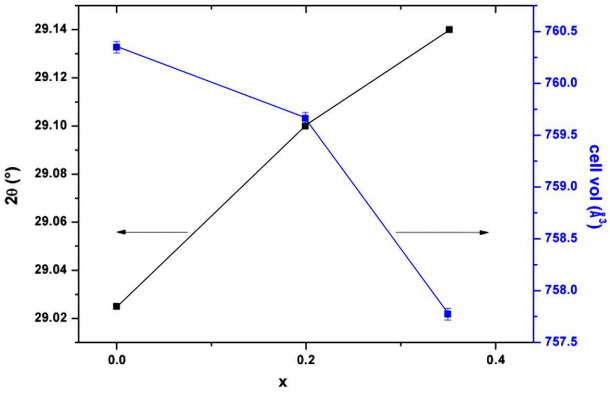


**Figure 2. $2\theta$ position of 115 peak and unit cell volume as functions of Eu-ion content ($x$)**

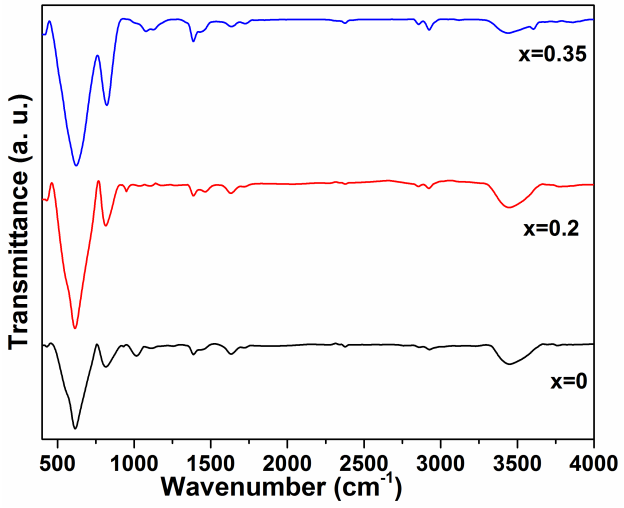


**Figure 3. FTIR spectra of $SrBi_{2-x}Eu_xNb_2O_9$ ceramic powders**

to be 7.29, 7.20 and 7.14 g/$cm^3$ for $x$ = 0, 0.2 and 0.35, respectively.

FTIR spectra of the $SrBi_{2-x}Eu_xNb_2O_9$ ceramic powders are shown in Fig. 3. The bands at ~3440, ~1382 and ~1630 $cm^{-1}$ are assigned to the O–H mode in $H_2O$ molecules. The C–H stretching band arising from contamination is present at ~2930 $cm^{-1}$. The bands at ~1090 and ~1400 $cm^{-1}$ reveal carbonate traces. The presence of two bands, approximately at ~620 and ~820 $cm^{-1}$, indicates Nb–O stretching of $NbO_6$ octahedron. These two bands are due to the lattice modes of $SrBi_2Nb_2O_9$ [12,13]. The band at ~430 $cm^{-1}$ occurs due to the oscillations of the Bi–O bond [14]. For the spectra of the Eu-doped $SrBi_{2-x}Eu_xNb_2O_9$, there are no additional shifts in the band or intensity.

Figure 4 shows the cross-section SEM images of the $SrBi_{2-x}Eu_xNb_2O_9$ ceramics. The images indicate that a material consists of one phase with well-bonded grains and a significant portion of porosity, especially for the doped samples (with $x$ = 0.2 and 0.35). The SEM of the undoped sample shows plate-like grains, which are typical characteristics for Aurivillius layered structures [15,16]. The sample doped with 35 at.% of Eu shows rod- and plate-shaped grains.

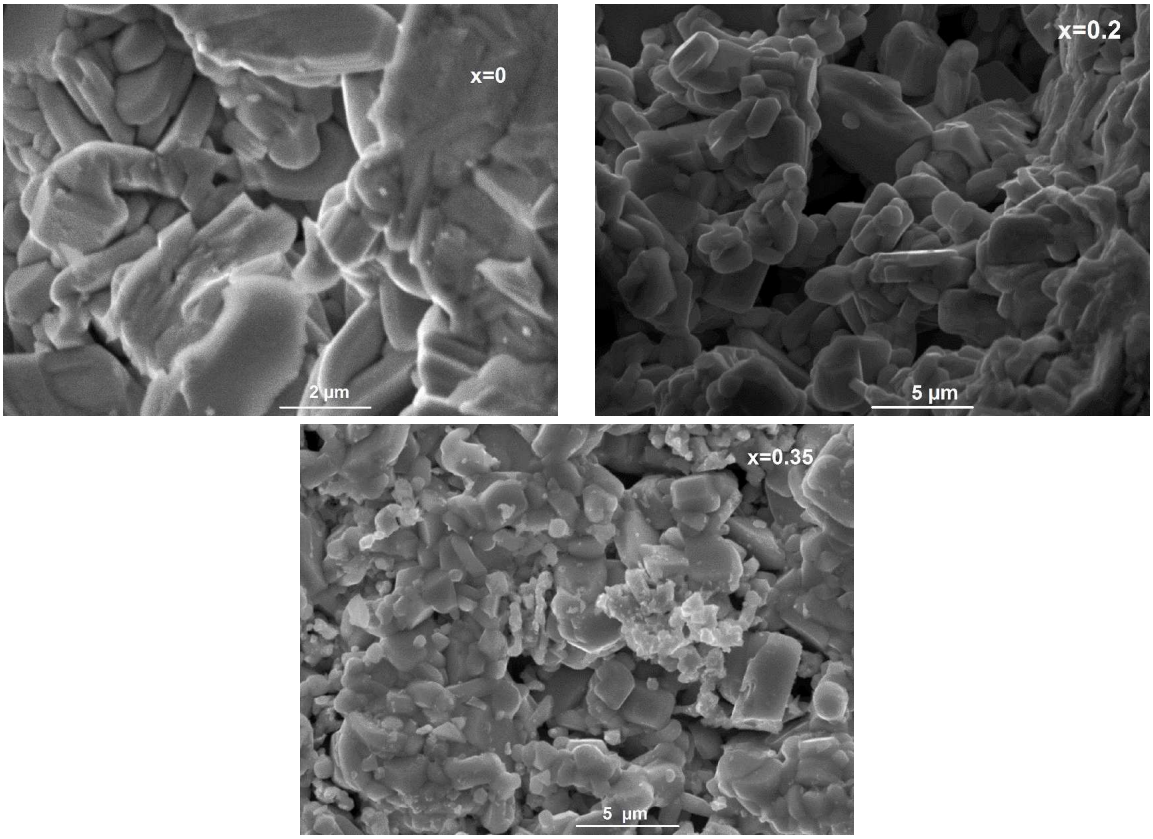


**Figure 4. SEM images of $SrBi_{2-x}Eu_xNb_2O_9$ ceramics**

### 3.2. Dielectric properties

Frequency dependence of the dielectric constant ($\varepsilon'$) and loss ($\tan\delta$) of the $SrBi_{2-x}Eu_xNb_2O_9$ ($x = 0, 0.2, 0.35$) ceramics at room temperature are shown in Fig. 5. At lower frequency, $\varepsilon'$ and $\tan\delta$ decrease with increasing frequency, usually due to the space charge polarization and interface effects, or lattice expansion [19]. Another explanation suggests that these observations may be due to the fact that the dipoles cannot follow the fast variation of the applied field. However, at higher frequency $\varepsilon'$ tends to be constant. This can be explained by the inability of electric dipoles to follow the fast variation of the alternating applied electric field. It is noticed from Table 1 that the sample with $x = 0$ possesses higher dielectric constant and loss ($\varepsilon'$, $\tan\delta$) than the Eu-doped samples. The dielectric loss significantly decreases from 0.04 for $x = 0$ to 0.02 and 0.006 for $x = 0.2$ and 0.35, respectively, when measured at 1 MHz. The room temperature conductivity of the undoped sample is found to be $20\times10^{-5}\ \Omega^{-1}\text{cm}^{-1}$, and decreases by Eu-doping about one order of magnitude (Table 1).

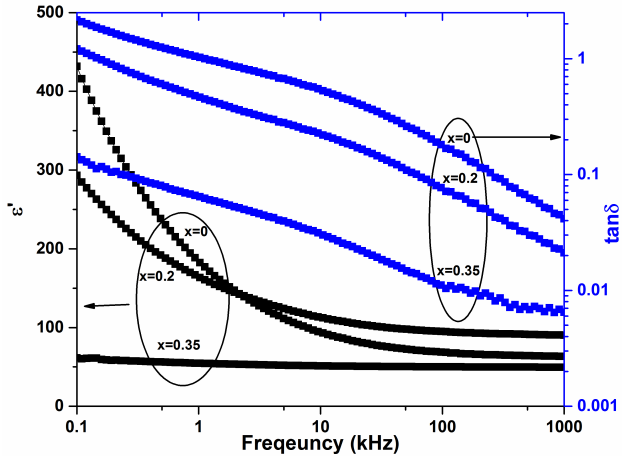


**Figure 5. Frequency dependence of dielectric constant ($\varepsilon'$) and dielectric loss ($\tan\delta$) of $SrBi_{2-x}Eu_xNb_2O_9$ ceramics**

Figure 6 shows the temperature dependence of the dielectric constant ($\varepsilon'$) and dielectric loss ($\tan\delta$) of the $SrBi_{2-x}Eu_xNb_2O_9$ ($x = 0, 0.2, 0.35$) ceramics at different frequencies. Both the Curie points and the peak dielectric constant decrease significantly with an increased

**Table 1. Electrical and dielectric properties of $SrBi_{2-x}Eu_xNb_2O_9$ ceramics at 1 MHz**

| Sample | Room temperature | | | $R_p$ |
|---|---|---|---|---|
| | $\varepsilon'$ | $\tan\delta$ | $\sigma$ [$10^{-5}\ \Omega^{-1}\text{m}^{-1}$] | [$10^5\ \Omega$] |
| $SrBi_2Nb_2O_9$ | 95 | 0.02 | 20 | 1.7 |
| $SrBi_{1.8}Eu_{0.2}Nb_2O_9$ | 63 | 0.04 | 7 | 7.7 |
| $SrBi_{1.65}Eu_{0.35}Nb_2O_9$ | 50 | 0.006 | 1.6 | 20 |

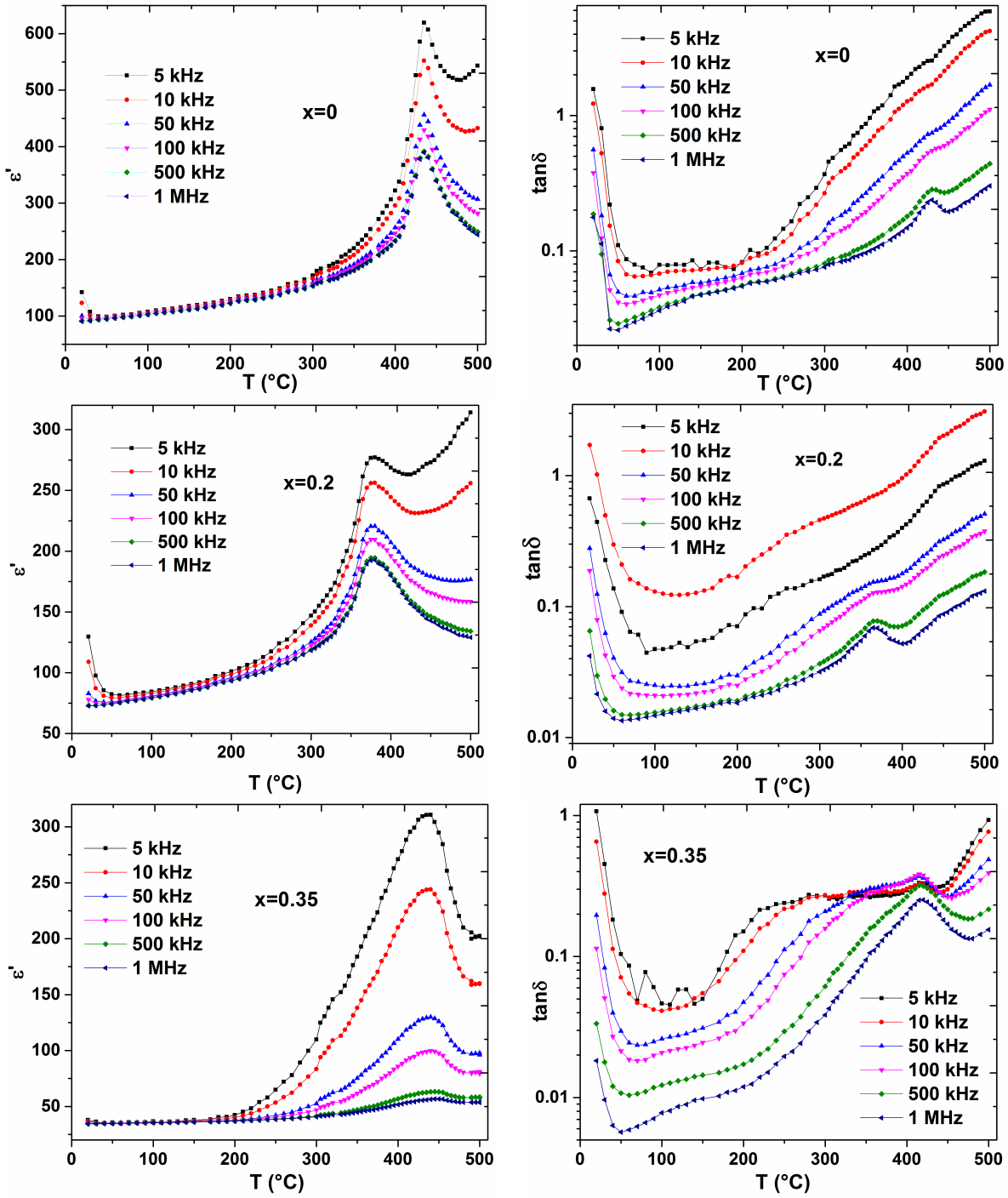


**Figure 6. Temperature dependence of dielectric constant ($\varepsilon'$)) and dielectric loss ($\tan\delta$) of $SrBi_{2-x}Eu_xNb_2O_9$ ceramics**

$Bi^{3+}$ substitution. Thus, the lattice compression occurring in the samples causes a decrease in the Curie temperature. The origin of ferroelectricity in bismuth layered ferroelectric materials (BLSFs) is linked to the tilting of the $BO_6$ octahedron [17]. Therefore, the difference in polarizability between $Bi^{3+}$ (6.04 Å$^3$) and $Eu^{3+}$ (4.53 Å$^3$) [18] may cause a reduction of dielectric constant measured at transition temperature.

Dielectric loss spectra reveal a broad dielectric loss peak appears close to the peak temperature of a dielectric constant, conforming ferroelectric-paraelectric phase transition.

The movement of the dielectric peak towards higher temperatures appearing at about 400 °C with increase of frequency is obvious for the sample with $x = 0.35$. This indicates on its relaxor behaviour. In this regard, the modified Curie-Weiss law [19] was used:

$$\ln\left(\frac{1}{\varepsilon'} - \frac{1}{\varepsilon'_m}\right) = \gamma \cdot \ln(T - T_m) \qquad (2)$$

where $\varepsilon'_m$ is the maximum value of dielectric permittivity at the transition temperature ($T_m$) and $\gamma$ is the diffuseness exponent ($1 \leq \gamma \leq 2$). Figure 7 shows the fitting

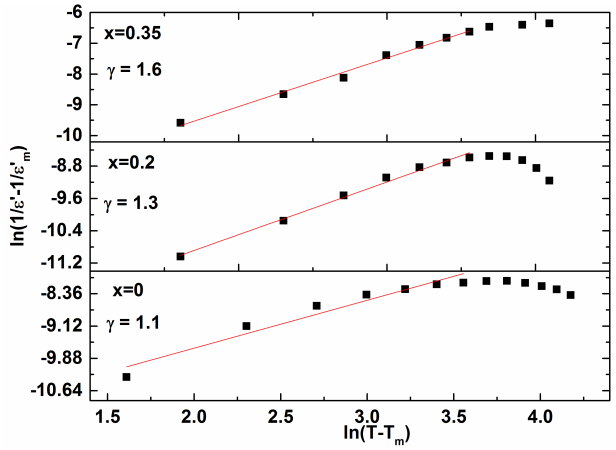


**Figure 7. $\ln(1/\varepsilon' - 1/\varepsilon'_m)$ versus $\ln(T - T_m)$ for $SrBi_{2-x}Eu_xNb_2O_9$ ceramics**

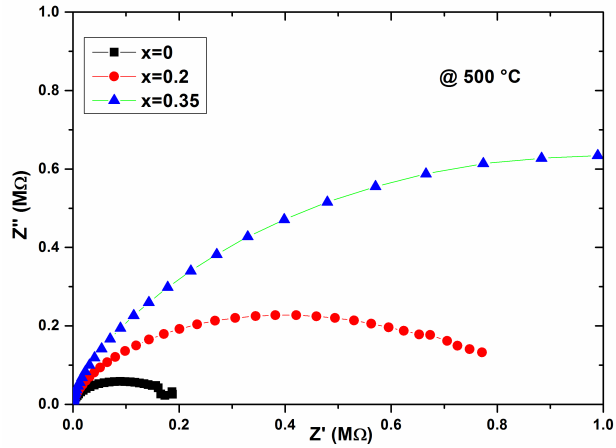


**Figure 8. Impedance spectra for $SrBi_{2-x}Eu_xNb_2O_9$ ceramics obtained at 500 °C**

done in accordance to the modified Curie-Weiss law for the paraelectric phase of the $SrBi_{2-x}Eu_xNb_2O_9$ ceramics. The obtained values of $\gamma$ increase from 1.1 for the undoped sample to 1.6 for the doped ones indicating a deviation from the normal to relaxor ferroelectric transition with introducing $Eu^{3+}$ ions into lattice structure.

Several studies investigated microstructure-grain boundary properties correlations as it was demonstrated that the physical properties of material strongly depend on the microstructure [20,21]. Further, the effect of the doping on dielectric properties is also very important and could support the statement that the relaxation phenomena of the Eu-doped samples might be reasonably attributed to the random distribution of $Eu^{3+}$ cations in the structure. Similarly, random distribution of Nd cations in $Na_{0.5}Nd_xBi_{2.5-x}Nb_2O_9$ structure was demonstrated by Long *et al.* [22]. They confirmed by the Rietveld refinement and Raman spectroscopy that Nd occupied both the A site in the perovskite layers and the cation site in the $(Bi_2O_2)^{2+}$ layers. The suggestion that the relative size of the cations is critical in determining disorder degree was supported by the work of Kennedy *et al.* [23], where they investigated disordering in $Pb_{1-x}Sr_xBi_2Nb_2O_9$ structure. A similar study was performed by Lei *et al.* [9]. In their work, the Curie temperature of $Sr_{1-x}Eu_xBi_2Nb_2O_9$ ceramics changes slightly when the concentration of the $Eu^{3+}$ is in the range of 0–0.6 at.%. They attributed a decrease in the Curie temperature to the lattice distortion, the electronic configuration, electronegativity and amount of $Bi^{3+}$ ions. Thus, in our case, random distribution of $Eu^{3+}$ ions between pseudo-perovskite ($SrNb_2O_7$) and ($Bi_2O_2$) layers may be the main reason for the observed relaxor behaviour of the sample $SrBi_{1.65}Eu_{0.35}Nb_2O_9$ [1,24,25].

The Nyquist plots of $SrBi_{2-x}Eu_xNb_2O_9$ obtained at 500 °C are shown in Fig. 8. The circuit is simulated with the parallel resistor and capacitor with contact resistor:

$$Z(\omega) = R_s + \frac{R}{(\omega \cdot R \cdot C)^2 + 1} - i\frac{\omega \cdot R^2 \cdot C}{(\omega \cdot R \cdot C)^2 + 1} \quad (3)$$

The impedance spectrum is characterized with the appearance of one semicircular arc over the entire experimental frequency range. A single semicircle confirms the presence of bulk effect in the materials [26]. The evolution of the circuit equivalent with dopants has been studied in a number of other $SrBi_2Nb_2O_9$ systems and they show only one semicircle [16,27]. The impedance data did not fit well with RC circuit, but rather this fitted with equivalent circuits containing one CPE (Constant Phase Element). The diameter of the semicircles increases significantly with increased amount of Eu. The $Z''$ *vs.* $Z'$ plot for the sample with $x = 0$ gives the signature of an arc. However, the sample with $x = 0.35$ shows an incomplete semicircle. This phenomenon may be attributed to the change of the pore structure of ceramics, as can be seen in many works dealing with the microstructure-impedance arc correlations [28–30].

## IV. Conclusions

In this paper, strontium bismuth niobate ($SrBi_2Nb_2O_9$) powders doped with Eu (0, 20 and 35 at.% Eu) were synthesized by solid-state method and sintered at 1130 and 1230 °C. The microstructure and electrical properties were investigated. XRD and SEM results confirm that the fabricated samples have the orthorhombic structure with rod- and plate-like grains typical for Aurivillius layered structures. FTIR spectra show a similarity between three samples. Dielectric measurements show that the dielectric loss of the Eu-doped ceramics is lower than that of the pure $SrBi_2Nb_2O_9$, whereas the relaxation behaviour is more expressed with the increase of Eu-addition. The impedance arc is found to be influenced by grain size and porosity.

## References

1. R. Qiu, F. Zhang, S. Zheng, Y. Li, W. Zhang, "Structural stability in Aurivillius phases based on ab initio thermodynamics", *J. Phys. Chem. Solids*, **75** (2014) 1088–1093.
2. P. Yang, "Fatigue behavior of $SrBi_2(Ta,Nb)_2O_9$ ferroelectric thin films fabricated by pulsed laser deposition",

*J. Mater. Sci. Mater. Electron.*, **17** (2006) 925–929.
3. I. Coondoo, A. K. Jha, S.K. Agarwal, "Structural, dielectric and electrical studies in tungsten doped $SrBi_2Ta_2O_9$ ferroelectric ceramics", *Ceram. Int.*, **33** (2007) 41–47.
4. B.R. Kannan, B.H. Venkataraman, "Influence of samarium doping on structural and dielectric properties of strontium bismuth tantalate ceramics derived by molten salt synthesis route", *J. Mater. Sci. Mater. Electron.*, **25** (2014) 4943–4948.
5. M. Afqir, A. Tachafine, D. Fasquelle, M. Elaatmani, J. Carru, A. Zegzouti, M. Daoud, "Synthesis, structural and dielectric properties of Ho-doped $SrBi_2Nb_2O_9$ prepared by co-precipitation method", *Sci. China Mater.*, **59** (2016) 921–926.
6. M. Afqir, A. Tachafine, D. Fasquelle, M. Elaatmani, J. Carru, A. Zegzouti, M. Daoud, "Structure and electric properties of cerium substituted $SrBi_{1.8}Ce_{0.2}Nb_2O_9$ and $SrBi_{1.8}Ce_{0.2}Ta_2O_9$ ceramics", *Process. Appl. Ceram.*, **10** [3] (2016) 183–188.
7. M. Afqir, A. Tachafine, D. Fasquelle, M. Elaatmani, A. Zegzouti, J.C. Carru, M. Daoud, "Synthesis, structural and dielectric properties of $SrBi_{2-x}Sm_xNb_2O_9$", *Moscow Univ. Phys. Bull.*, **72** (2017) 196–202.
8. D.P. Volanti, I.L. V Rosa, E.C. Paris, C.A. Paskocimas, P.S. Pizani, J.A. Varela, E. Longo, "The role of the $Eu^{3+}$ ions in structure and photoluminescence properties of $SrBi_2Nb_2O_9$ powders", *Opt. Mater.*, **31** (2009) 995–999.
9. L. Yu, J. Hao, Z. Xu, W. Li, R. Chu, G. Li, "Strong photoluminescence and good electrical properties in Eu-modified $SrBi_2Nb_2O_9$ multifunctional ceramics", *Ceram. Int.*, **42** (2016) 14849–14854.
10. S. Khasa, P. Singh, S. Sanghi, N. Singh, A. Agarwal, "Structural analysis and dielectric characterization of Aurivillius type $CaSrBi_2Nb_2O_9$ ceramics", *J. Integr. Sci. Technol.*, **2** (2014) 13–21.
11. R.D. Shannon, C.T. Prewitt, "Effective ionic radii in oxides and fluorides", *Acta Crystallogr. Sect. B Struct.*, **B25** (1969) 925–946.
12. M.J.S. da Rocha, M.C.C. Filho, K.R.B. Theophilo, J.C. Denardin, I.F. de Vasconcelos, E.B. de Araujo, A.S.B. Sombra, "Ferrimagnetism and ferroelectricity of the composite matrix: $SrBi_2Nb_2O_9(SBN)_X$-$BaFe_{12019}(BFO)_{100-X}$", *Mater. Sci. Appl.*, **3** (2012) 6–17.
13. M.J.S. Rocha, P.M.O. Silva, K.R.B. Theophilo, E.O. Sancho, P.V.L. Paula, M. A. S. Silva, S.B. Honorato, A.S.B. Sombra, "High dielectric permittivity in the microwave region of $SrBi_2Nb_2O_9$ (SBN) added $La_2O_3$, PbO and $Bi_2O_3$, obtained by mechanical alloying", *Phys. Scr.*, **86** (2012) 025701.
14. A.V. Egorysheva, V.I. Burkov, Y.F. Kargin, V.G. Plotnichenko, V.V. Koltashev, "Vibrational spectra of crystals of bismuth borates", *Crystallogr. Rep.*, **50** (2005) 127–136.
15. S.K. Patri, R.N.P. Choudhary, "Solid solutions of bismuth-based Aurivillius oxides: Structural and dielectric characterization", *Appl. Phys. A*, **94** (2009) 321–327.
16. B.H. Venkataraman, K.B.R. Varma, "Microstructural, dielectric, impedance and electric modulus studies on vanadium-doped and pure strontium bismuth niobate ($SrBi_2Nb_2O_9$) ceramics", *J. Mater. Sci. Mater. Electron.*, **16** (2005) 335–344.
17. Z.H. Duan, K. Jiang, L.P. Xu, Y.W. Li, Z.G. Hu, J.H. Chu, "Intrinsic relationship between electronic structures and phase transition of $SrBi_{2-x}Nd_xNb_2O_9$ ceramics from ultraviolet ellipsometry at elevated temperatures", *J. Appl. Phys.*, **115** (2014) 054107.
18. R.D. Shannon, "Dielectric polarizabilities of ions in oxides and fluorides", *J. Appl. Phys.*, **73** (1993) 348–366.
19. X. Zhu, X.-M. Chen, "Ferroelectric transition and Curie-Weiss behavior in some filled tungsten", *Chinese Phys. Lett.*, **31** (2014) 015201.
20. B.B. Straumal, A.A. Mazilkin, S.G. Protasova, S.V. Stakhanova, P.B. Straumal, M.F. Bulatov, G. Schutz, T. Tietze, E. Goering, B. Baretzky, "Grain boundaries as a source of ferromagnetism and increased solubility of Ni in nanograined ZnO", *Rev. Adv. Mater. Sci.*, **41** (2015) 61–71.
21. B.B. Straumal, S.G. Protasova, A.A. Mazilkin, E. Goering, G. Schütz, P.B. Straumal, B. Baretzky, "Ferromagnetic behaviour of ZnO: The role of grain boundaries", *Beilstein J. Nanotechnol.*, **7** (2016) 1936–1947.
22. C. Long, H. Fan, P. Ren, "Structure, phase transition behaviors and electrical properties of Nd substituted Aurivillius polycrystallines $Na_{0.5}Nd_xBi_{2.5-x}Nb_2O_9$ (x = 0.1, 0.2, 0.3, and 0.5)", *Inorg. Chem.*, **9** (2013) 5045–5054.
23. B.J. Kennedy, B.A. Hunter, "Cation disorder in Pb-doped $SrBi_2Nb_2O_9$", *Chem. Mater.*, **13** (2001) 4612–4617.
24. A. Khokhar, P.K. Goyal, O.P. Thakur, K. Sreenivas, "Effect of excess of bismuth doping on dielectric and ferroelectric properties of $BaBi_4Ti_4O_{15}$ ceramics", *Ceram. Int.*, **41** (2015) 4189–4198.
25. M. Dolgos, U. Adem, X. Wan, Z. Xu, A. J. Bell, T.P. Comyn, T. Stevenson, J. Bennett, J.B. Claridge, M.J. Rosseinsky, "Chemical control of octahedral tilting and off-axis A cation displacement allows ferroelectric switching in a bismuth-based perovskite", *Chem. Sci.*, **3** (2012) 1426.
26. J.R. Macdonald, "Impedance spectroscopy and its use in analyzing the steady-state ac response of solid and liquid electrolytes", *J. Electroanal. Chem.*, **223** (1987) 25–50.
27. K.S. Rao, D.M. Prasad, P.M. Krishna, B.H.B. Suneetha, K. Suneetha, "Frequency and temperature dependence of electrical properties of barium and gadolinium substituted $SrBi_2Nb_2O_9$ ceramics", *J. Mater. Sci.*, **42** (2007) 7363–7374.
28. M.L. Dunn, M. Taya, "Electromechanical properties of porous piezoelectric ceramics", *J. Am. Ceram. Soc.*, **76** (1993) 1697–1706.
29. C. Hitz, A. Lasia, "Experimental study and modeling of impedance of the her on porous Ni electrodes", *J. Electroanal. Chem.*, **500** (2001) 213–222.
30. H. Wang, J. Liu, J. Zhai, B. Shen, Z. Pan, K. Yang, J. Liu, "Effect of $K_2O$ content on breakdown strength and energy-storage density in $K_2O$-BaO-$Nb_2O_5$-$SiO_2$ glass-ceramics", *Ceram. Int.*, **43** (2017) 4183–4187.